Proc. Natl. Acad. Sci. USA
Vol. 84, pp. 896–900, February 1987
Physiological Sciences

Na^+ channels as sites of action of the cardioactive agent DPI 201-106 with agonist and antagonist enantiomers

(cardiac cell/neuroblastoma cell/voltage-clamp/binding/flux experiment)

G. ROMEY*, U. QUAST†, D. PAURON*, C. FRELIN*, J. F. RENAUD*, AND M. LAZDUNSKI*‡

*Centre de Biochimie, Centre National de la Recherche Scientifique, Parc Valrose, 06034 Nice Cedex, France; and †Laboratories Sandoz, Division Pharmaceutique, Recherches Pré-Cliniques, CH-4002 Basel, Switzerland

Communicated by Pierre Joliot, October 6, 1986

ABSTRACT **This paper shows the interaction of the cardiotonic agent 4-[3-(4-diphenylmethyl-1-piperazinyl)-2-hydroxypropoxy]-1*H*-indole-2-carbonitrile (DPI 201-106) and its optic enantiomers *R*-DPI (205-429) and *S*-DPI (205-430) with the Na^+ channel of a variety of excitable cells. Voltage-clamp experiments show that DPI 201-106 acts on neuroblastoma cells and rat cardiac cells. *S*-DPI (205-430) increases the peak Na^+ current, slows down the kinetics of Na^+ channel inactivation, and is cardiotonic on heart cells. Conversely, *R*-DPI (205-429) reduces the peak Na^+ current and blocks Na^+ channel activity and cardiac contractions. Binding experiments using radioactively labeled toxins indicate that DPI 201-106 and its enantiomers do not interact with sites already identified for tetrodotoxin or sea anemone and scorpion toxins. DPI 201-106 and its enantiomers inhibit binding of a ^3H-labeled batrachotoxin derivative, [^3H]batrachotoxinin A 20-α-benzoate, to brain membranes. The dissociation constant of the complex formed between the Na^+ channel and both *R*-DPI and *S*-DPI is $K_d \simeq$ 100 nM. $^{22}Na^+$ uptake experiments using different cell types have shown that *R* and *S* enantiomers of DPI 201-106 are active on the different Na^+ channel subtypes with similar IC_{50} values. These results are discussed in relation with the cardiotonic properties of DPI 201-106 that are not accompanied by cardiotoxic effects.**

4-[3-(4-Diphenylmethyl-1-piperazinyl)-2-hydroxypropoxy]-1*H*-indole-2-carbonitrile (DPI 201-106) is a cardiotonic agent currently used in clinical trials for the therapy of congestive heart failure (30). The positive inotropic effect of DPI appears to be due to an effect of the drug on the myocardial Na^+ channel (1–3).

The Na^+ channel is the target of a variety of neurotoxins. These toxins have different modes of action and different binding sites (4–7). Sites that are best identified are those for (*i*) tetrodotoxin (TTX) and saxitoxin, (*ii*) batrachotoxin (BTX) and veratridine, (*iii*) scorpion and sea anemone toxins, which, similarly to DPI, prolong action potentials by slowing down inactivation and have cardiotonic effects, and (*iv*) other scorpion toxins that alter the activation process of the Na^+ channel.

The purpose of this paper is to analyze the mechanism by which DPI acts on the Na^+ channel with the particular purpose to answer the following questions: Is the action of the drug specific to the cardiac Na^+ channel? What is the binding site of DPI on the Na^+ channel? Is it one of the previously identified binding sites for natural toxins? Are there differences in the action mechanism of the different DPI enantiomers?

The publication costs of this article were defrayed in part by page charge payment. This article must therefore be hereby marked "*advertisement*" in accordance with 18 U.S.C. §1734 solely to indicate this fact.

MATERIALS AND METHODS

Chemicals and Toxins. DPI 201-106 and its optic enantiomers *R*-DPI (205-429) and *S*-DPI (205-430) (purity > 97%) were provided by Sandoz. TTX was purchased from Sankyo and its tritiated ethylenediamine derivative ([^3H]en-TTX, 25 Ci/mmol; 1 Ci = 37 GBq) was synthetized as described (8). Toxin γ from *Tityus serrulatus* venom (TiTxγ) and BTX were gifts from J. R. Giglio and J. W. Daly, respectively. Toxins II and V from the sea anemone *Anemonia sulcata* (AS_{II} and AS_V) and toxin II from the scorpion *Androctonus australis* (AaH_{II}) were purified in our laboratory by H. Schweitz. TiTxγ and AaH_{II} were iodinated by the lactoperoxidase/H_2O_2 method (9) and AS_V was iodinated according to ref. 10. [^3H]Batrachotoxinin A 20-α-benzoate ([^3H]BTXB) was from New England Nuclear. Veratridine, tetracaine, ouabain, and *Leiurus quinquestriatus* scorpion venom were from Sigma, and aconitine was from Roth.

Membrane Preparations and Cell Cultures. Rat brain synaptosomes and guinea pig brain cortical vesicular preparations were isolated as described (11, 12). Primary cultures of rat skeletal myoblasts, chicken and rat cardiac cells, and cells of the N1E 115 neuroblastoma cell line and of the C_9 cell line were prepared and grown as described (13).

Binding Experiments. Equilibrium binding of the different labeled toxins to the Na^+ channel was measured according to ref. 14 for [^3H]en-TTX, according to ref. 10 for ^{125}I-labeled AS_V and AaH_{II} (^{125}I-AS_V and ^{125}I-AaH_{II}), and according to ref. 15 for ^{125}I-labeled TiTxγ (^{125}I-TiTxγ). [^3H]BTXB specific binding to synaptosomes was determined in the presence of 0.1 mM AS_{II} or 0.12 mg of crude *L. quinquestriatus* scorpion venom per ml. After 2 hr of incubation at 4°C or 37°C, incubation media were filtered onto polyethyleneimine-treated GF/B glass fiber filters (16). Nonspecific binding of [^3H]BTXB was determined in the presence of 0.2 mM aconitine.

Electrophysiology. Intracellular recordings on rat cardiac cells cultured in the form of monolayers were performed by means of conventional glass microelectrodes as described (17). The temperature of the culture dish was maintained at 35–36°C. Spontaneous beating rates and amplitudes of contractions were recorded simultaneously with the electrical activity and analyzed with the combination of a Sony TV camera and a simplified real-time TV image analyzer based on an Apple II microcomputer (18). Isolated rat embryonic cardiac cells and N1E 115 neuroblastoma cells were voltage-

Abbreviations: DPI 201-106, 4-[3-(4-diphenylmethyl-1-piperazinyl)-2-hydroxypropoxy]-1*H*-indole-2-carbonitrile; TTX, tetrodotoxin; [^3H]en-TTX, [^3H]ethylenediamine-TTX; BTX, batrachotoxin; [^3H]BTXB, [^3H]batrachotoxinin A 20-α-benzoate; TiTxγ, toxin γ from *Tityus serrulatus* venom; AS_{II} and AS_V, toxins II and V from the sea anemone *Anemonia sulcata*; AaH_{II}, toxin II from the scorpion *Androctonus australis*.

‡To whom reprint requests should be addressed.

clamped at 20°C by the whole-cell variant of the patch-clamp technique described by Hamill *et al.* (19). The culture medium was replaced by an external solution containing 120 mM NaCl, 25 mM tetraethylammonium chloride, 1.8 mM $CaCl_2$, 0.4 mM $MgCl_2$, and 5 mM glucose. This solution was buffered at pH 7.4 with 25 mM Hepes/tetramethylammonium hydroxide and its osmolarity was adjusted with sucrose to 300 mosM. The pipette solution contained 140 mM CsCl, 5 mM EGTA, and 10 mM Hepes buffered at pH 7.2 with CsOH. Patch pipettes (≈2 MΩ) were connected to the head stage of the recording apparatus (RK 300, Biologic, Grenoble, France). The signal was low-pass filtered at 5 kHz, sampled at 25 kHz, and stored and analyzed with a minicomputer system (Plessey systems model 6220, Irvine, CA).

$^{22}Na^+$ Flux Experiments. Flux experiments were carried out by using previously described techniques (13).

RESULTS

Effects on Cardiac Contractions and Electrophysiological Analysis of the Action Mechanism of DPI 201-106 and *R*- and *S*-DPI. Fig. 1 *A* and *B* shows that DPI 201-106 and its optic enantiomer *S*-DPI have similar effects on electrical and mechanical activities of rat cardiac cells in culture. They cause a significative prolongation of the action potential, a reduction of the beating rate, and a net increase of the contraction. Recordings over a period of 30 min do not show any evidence for an arythmogenic effect. In comparison, the application of AS_{II}, a sea anemone toxin that prolongs the action potential duration in a variety of preparations by specifically slowing down the Na^+ inactivation process (20), provokes larger (but similar) effects on the action potential duration and similar effects on the amplitude of contraction (Fig. 1*C*). Unlike DPI 201-106 and *S*-DPI, AS_{II} causes a very significant arrhythmia.

Application of *R*-DPI progressively decreased the amplitude of the action potential and ultimately blocked spontaneous contractions (Fig. 1*D*).

The effects of the two enantiomers were analyzed by voltage-clamp experiments using two different cellular types: single rat heart cells in culture, which are TTX-resistant (21), and N1E 115 neuroblastoma cells, which are TTX-sensitive (13).

Application of *R*-DPI (1 μM) to rat cardiac cells (five experiments) led, in all cases, to a progressive decrease of the Na^+ current amplitude without changes in the current kinetics. After 10 min, the peak Na^+ current was reduced to about 10% of its control value (Fig. 2*A*). Conversely, application of *S*-DPI (1 μM) for 5 min on the same type of preparation (six experiments) led to an increase of about 40% of the peak Na^+ current and a slowing down of the kinetics of Na^+ channel inactivation (Fig. 2*B*).

Effects of *R*- and *S*-DPI on the Na^+ current of N1E 115 neuroblastoma cells were similar to those found in rat cardiac cells. The Na^+ current was 70% blocked after application of 1 μM *R*-DPI and totally blocked after a 5-min application of 10 μM *R*-DPI (10 experiments) (Fig. 2*C*). Conversely, *S*-DPI (10 μM) always slowed down Na^+ channel inactivation in neuroblastoma cells (seven experiments) (Fig. 2*D*) as it did in cardiac cells (Fig. 2*B*). The blocking effect of *R*-DPI predominates on both preparations after the application of a mixture of the two enantiomers containing 1 μM *S*-DPI and 10 μM *R*-DPI (data not shown).

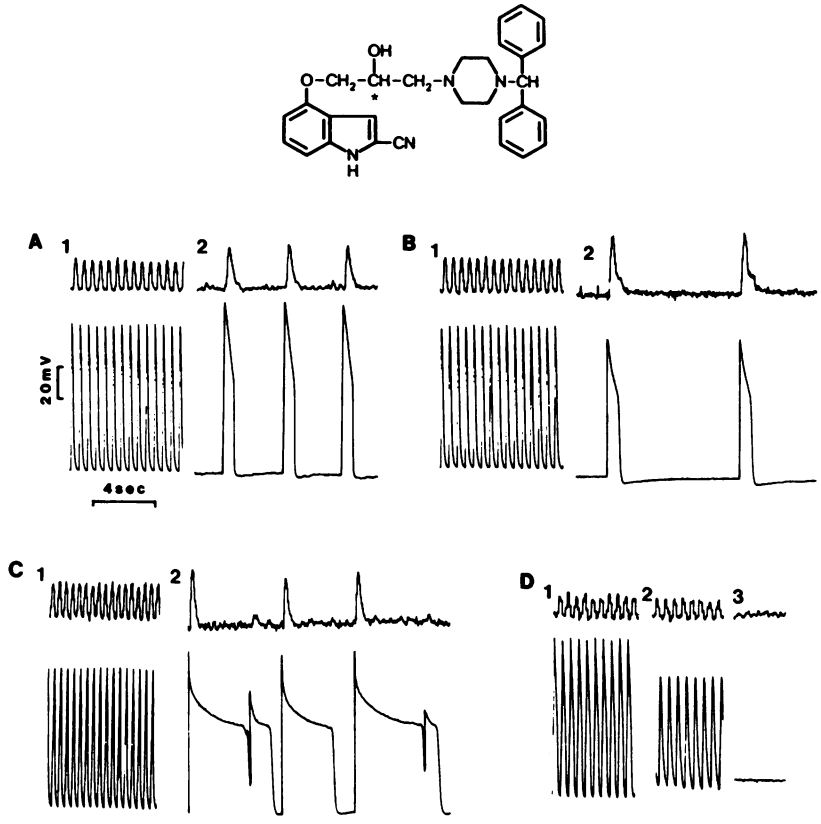

FIG. 1. (*Upper*) Chemical structure of DPI 201-106, which is a racemic 1:1 mixture of the *R* enantiomer 205-429 and the *S* enantiomer 205-430. An asterisk (*) marks the asymmetric carbon. (*Lower*) Comparative effects of DPI 201-106, of its optic enantiomers *S*- and *R*-DPI, and of the sea anemone toxin AS_{II} on the electrical (bottom traces) and mechanical (top traces) activities of rat cardiac cells cultured for 3 days in monolayers. (*A*) 1: Control. 2: Five minutes after the addition of 5 μM DPI 201-106. (*B*) 1: Control. 2: Five minutes after the addition of 1 μM *S*-DPI. (*C*) 1: Control. 2: Four minutes after the addition of 20 nM AS_{II}. (*D*) 1: Control. 2 and 3: Five minutes (2) and 10 min (3) after the addition of 1 μM *R*-DPI.

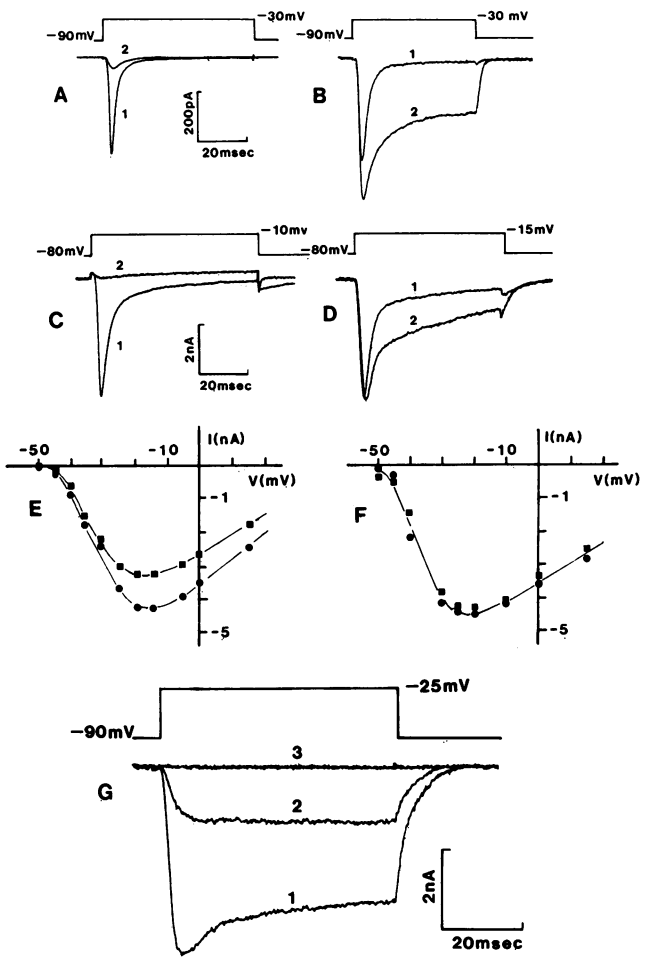

FIG. 2. (*A* and *B*) Na^+ current records from isolated rat cardiac cells in culture. (*A*) 1: Control. 2: After a 10-min application of 1 μM *R*-DPI. (*B*) 1: Control. 2: After a 5-min application of 1 μM *S*-DPI. (*C* and *D*) Na^+ current records from N1E 115 neuroblastoma cells. (*C*) 1: Control. 2: After a 5-min application of 10 μM *R*-DPI. (*D*) 1: Control. 2: After a 6-min application of 10 μM *S*-DPI. (*E* and *F*) N1E 115 neuroblastoma cells: peak Na^+ current–membrane potential relationships. ●, Control currents; ■, steady-state effects of 1 μM *R*-DPI (*E*) and 10 μM *S*-DPI (*F*). (*G*) Suppression of the S-DPI-induced Na^+ current by TTX in N1E 115 neuroblastoma cells. 1: Control after a 10-min incubation with 10 μM *S*-DPI. 2 and 3: Three minutes (2) and 10 min (3) after the addition of 0.1 μM TTX.

Na^+ current traces recorded in neuroblastoma cells at different voltage test pulses show that the application of *R*-DPI (Fig. 2*E*) and of *S*-DPI (Fig. 2*F*) had no appreciable effect on the membrane potential dependence of the peak Na^+ current. The activation of Na^+ currents slowed after *S*-DPI treatment, particularly at low membrane potential between −50 and −30 mV. TTX (0.1 μM), which blocks Na^+ current in neuroblastoma cells, also blocks the *S*-DPI-modified Na^+ current (Fig. 2*G*).

Effects of DPI 201-106 and of Its Optic Enantiomers *R*-DPI and *S*-DPI on the Specific Binding of Different Toxins Specific of the Voltage-Dependent Na^+ Channel to Brain Membranes. The *Inset* of Fig. 3*A* shows that 10 μM DPI does not modify [^{3}H]en-TTX binding, barely modifies ^{125}I-AS$_V$ and ^{125}I-TiTxγ binding, and enhances the binding of ^{125}I-AaH$_{II}$ to rat brain synaptosomes. Further experiments demonstrated that, as reported for BTX (22), high concentrations (30 μM) of *R*-DPI and of *S*-DPI enhance the specific ^{125}I-AaH$_{II}$ binding to synaptosomes by 2-fold (data not shown). Conversely, the main panel of Fig. 3*A* illustrates that DPI fully inhibits [^{3}H]BTXB binding to these membranes in a dose-dependent manner. The concentration of DPI that inhibits 50% of the

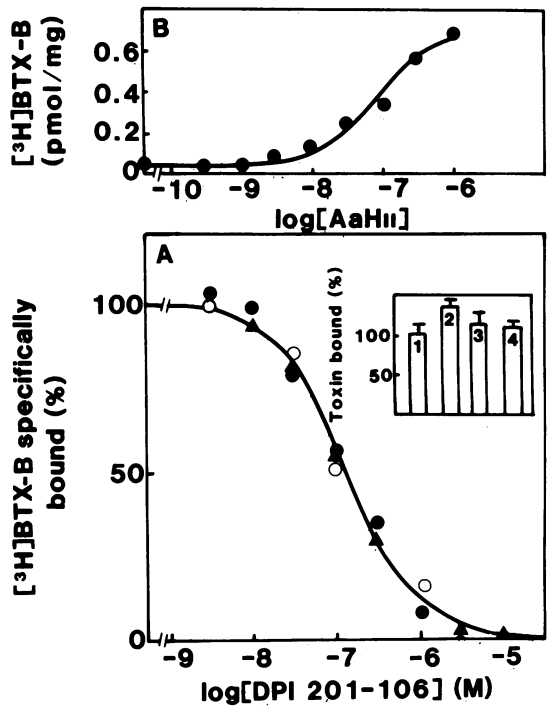

FIG. 3. (*A*) Inhibition of [^{3}H]BTXB binding to synaptosomes by DPI 205-429 (○), DPI 205-430 (●), and DPI 201-106 (▲). Synaptosomes (1.6 mg of protein per ml) were incubated at 4°C for 10 min with various concentrations of each compound. The amount of [^{3}H]BTXB specifically bound was measured after 2 hr of incubation in the presence of 14 nM [^{3}H]BTXB and 1 μM unlabeled AS$_{II}$. Maximal binding (100%) was 96 fmol of [^{3}H]BTXB bound per mg of protein. (*Inset*) Effects of DPI 201-106 on the binding of other neurotoxins acting on the Na^+ channel: TTX (1), AaH$_{II}$ (2), AS$_V$ (3), TiTxγ (4). Ten micromolar DPI 201-106 was incubated at 4°C with synaptosomes before adding the labeled toxins. Error bars indicate the standard deviation of the mean. (*B*) Enhancement of [^{3}H]BTXB specific binding to synaptosomes by AaH$_{II}$. [^{3}H]BTXB (15 nM) was incubated with synaptosomes (1.6 mg of protein per ml) and increasing concentrations of AaH$_{II}$. The radioactivity bound to synaptosomes was measured after incubation for 2 hr at 4°C. Nonspecific binding was determined in the presence of 0.2 mM veratridine.

specific [^{3}H]BTXB binding, $K_{0.5}$, is 140 nM. The same value is found for *R*-DPI and *S*-DPI. Very similar results were obtained for the guinea pig brain preparation at 37°C, where the $K_{0.5}$ values for DPI inhibition of the specific [^{3}H]BTXB binding were observed at 78 nM (*R*-DPI), 140 nM (*S*-DPI), and 130 nM (racemic DPI) (data not shown). Under these conditions it was observed that *R*-DPI was slightly more potent than *S*-DPI. Fig. 3*B* shows that AaH$_{II}$, which, like *S*-DPI, slows down Na^+ channel inactivation (23), increases [^{3}H]BTXB binding instead of inhibiting it.

Fig. 4 shows the results of equilibrium [^{3}H]BTXB binding experiments to guinea pig brain vesicles in the absence and presence of *R*- or *S*-DPI. Specific [^{3}H]BTXB binding shows no deviation from the simple Langmuir binding isotherm with K_d = 20 nM and B_{max} = 1.9 pmol/mg. The mean values from six experiments are K_d = 29 ± 1 nM and B_{max} = 2.0 ± 0.3 pmol/mg. In the presence of the *R* or *S* enantiomers of DPI, the Scatchard plots for the specific [^{3}H]BTXB binding remain linear, but it is seen that both enantiomers behave as mixed-type inhibitors of [^{3}H]BTXB binding, affecting mainly the K_d value but also the B_{max} value.

$^{22}Na^+$ Flux Experiments. $^{22}Na^+$ flux experiments with excitable and nonexcitable cells in culture have been widely used to analyze the pharmacological and biochemical properties of the TTX-blockable Na^+ channel (5, 6). DPI was unable to significantly increase the initial rate of $^{22}Na^+$ entry into any of the five cellular types used in this investigation—

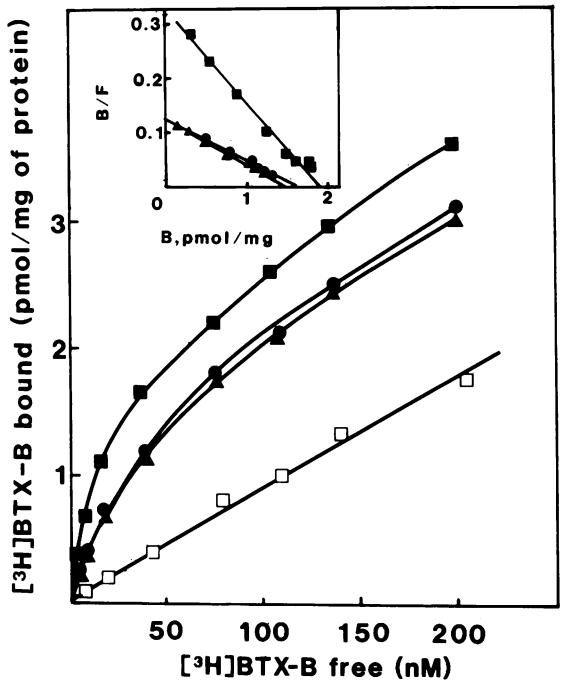

FIG. 4. Effect of *R*- and *S*-DPI on [^{3}H]BTXB binding. Experiments were performed with guinea pig brain vesicles (3.2 mg of protein per ml) at 37°C with 2 hr of incubation. ■, Total binding in the absence of DPI; ▲, *R*-DPI concentration = 0.2 μM; ●, *S*-DPI concentration = 0.40 μM; □, aconitine concentration = 0.2 mM (nonspecific binding). (*Inset*) Scatchard representation of specific binding. B/F, bound/free. Fit of specific binding to the law of mass action gave the following: ■, (no DPI) K_d = 20 ± 1 nM, B_{max} = 1.9 ± 0.1 pmol/mg of protein; ▲, K_d = 36 ± 4 nM, B_{max} = 1.4 ± 0.2 pmol/mg of protein; ●, K_d = 39 ± 2 nM, B_{max} = 1.5 ± 0.1 pmol/mg of protein.

i.e., N1E 115 neuroblastoma cells, rat skeletal muscle cells, rat and chicken cardiac cells, and C_9 cells—as illustrated for neuroblastoma cells in Fig. 5*A*. In that sense, DPI behaved like sea anemone toxin II (AS_{II}) and *A. australis* Hector toxin II (AaH_{II}). However, DPI was able to inhibit the component of $^{22}Na^+$ entry that was stimulated by veratridine, by BTX, or by a mixture of veratridine and AS_{II}, an effect that is similar to that observed with TTX.

Fig. 5*B* shows dose–response curves for DPI inhibition of $^{22}Na^+$ influx produced by application of BTX to neuroblastoma cells, rat muscle cells, and C_9 cells. It appears that the effect of DPI is the same in all cell types. Fig. 5*C* shows that *R*- and *S*-DPI both inhibit the $^{22}Na^+$ influx component, passing through the toxin-activated Na^+ channel in N1E 115 neuroblastoma cells with identical IC_{50} values (1 μM). Knowing that DPI inhibits the association of BTX to its receptor site (Fig. 4) and presumably, in the same way, the association of veratridine (which binds to the same site as BTX), one can easily pass from the IC_{50} value to the true "functional" dissociation constant K_d using the following equation: $IC_{50} = K_d \cdot (1 + [BTX]/K_{d(BTX)})$. Using this equation and a $K_{d(BTX)}$ of 10 μM, the K_d value for DPI is 120 nM.

Fig. 5*C* also shows (*i*) that $^{22}Na^+$ flux in chicken and rat cardiac cells is similarly inhibited by DPI enantiomers and (*ii*) that the dose–response curves for the action of *R*- and *S*-DPI are nearly the same.

DISCUSSION

Because digitalis action is accompanied by toxic effects and because the therapeutic index of this category of cardiotonic molecules is low (24), there is an increased interest in finding additional drugs that can be useful for the treatment of congestive heart failure.

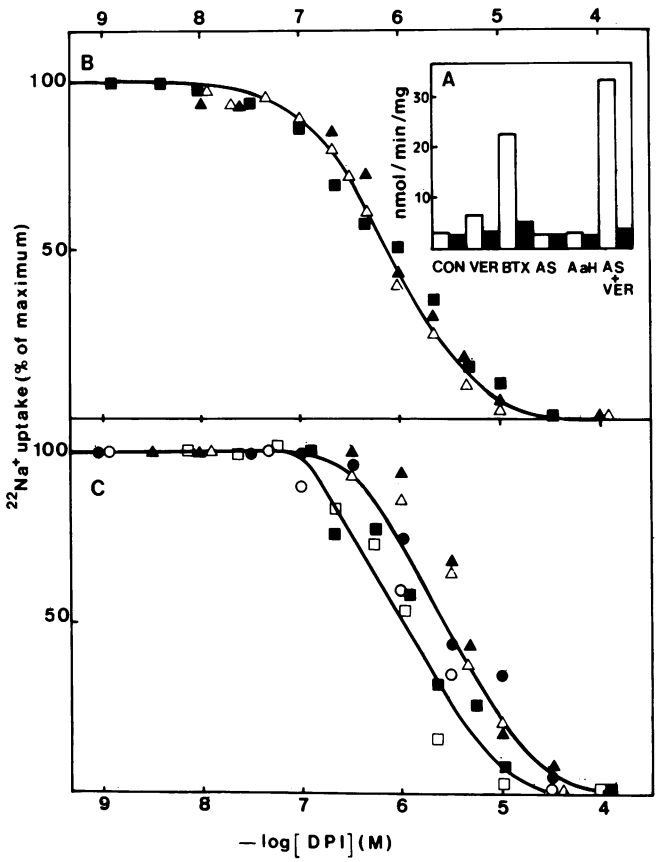

FIG. 5. Inhibition by DPI of toxin-activated $^{22}Na^+$ uptake in various cell types. (*A*) Influence of DPI 201-106 on the initial rate of $^{22}Na^+$ uptake by N1E 115 neuroblastoma cells. Experiments were performed in the absence of neurotoxin (CON) or in the presence of 0.1 mM veratridine (VER), 10 μM BTX, 10 μM AS_{II} (AS), 10 μM AaH_{II} (AaH), or a mixture of 0.1 mM veratridine and 10 μM AS_{II} (AS + VER). DPI 201-106 was used at 10 μM (solid bars). (*B*) Dose–response curves for DPI 201-106 inhibition of the rate of $^{22}Na^+$ uptake by N1E 115 neuroblastoma cells (■), C_9 cells (△), and rat skeletal myoblasts (▲). Toxin used was 10 μM BTX. (*C*) Dose–response curves for *R*-DPI (▲, ●, ■) and *S*-DPI (△, ○, □) inhibition of the rate of $^{22}Na^+$ uptake by chicken cardiac cells (▲, △), rat cardiac cells (●, ○), and N1E 115 neuroblastoma cells (■, □). Toxin used was 10 μM BTX.

The piperazinyl-indole DPI 201-106, which is a racemic mixture, and the *S*-enantiomeric form DPI 205-430 are strongly cardiotonic (Fig. 1) (30). The primary target of DPI 201-106 is the cardiac voltage-dependent Na^+ channel (1, 2). DPI slows down the inactivation of the channel (refs. 2 and 3 and Fig. 2). Voltage-clamp experiments presented in Fig. 2 show that *S*-DPI acts similarly on TTX-resistant Na^+ channels of rat cardiac cells and on TTX-sensitive Na^+ channels of neuroblastoma cells.

Electrophysiological measurements have revealed the very interesting fact that *S*-DPI tends to act as a Na^+ channel agonist, whereas *R*-DPI tends to act as a Na^+ channel antagonist and blocks spontaneous contractions in heart cells. This situation is similar to that found among effectors of the voltage-dependent Ca^{2+} channel in the 1,4-dihydropyridine family. It has been found that the two enantiomers of the same 1,4-dihydropyridine molecule have opposite effects on Ca^{2+} channel activity. (−)-Bay K8644 and (+)-202-791 are Ca^{2+} channel activators, whereas (+)-Bay K8644 and (−)-202-791 are Ca^{2+} channel blockers (25, 26). Binding experiments to brain membranes involving the TTX derivative [^{3}H]en-TTX, the scorpion toxin ^{125}I-AaH_{II}, the sea anemone toxin ^{125}I-AS_V, and the scorpion toxin ^{125}I-TiTxγ have clearly shown that DPI does not bind to any of the

specific sites normally occupied by these different toxins on the Na^+ channel structure. DPI even favors a 30% increase in binding of AaH_{II} (Fig. 3*A Inset*). The only binding that is negatively affected by DPI is that of [^{3}H]BTXB (Fig. 3*A*). This DPI effect is clearly different from that of the scorpion toxin AaH_{II}, which favors [^{3}H]BTXB binding (Fig. 3*B*), as observed with another toxin having the same mechanism of action (27).

R- and *S*-DPI do not bind to the BTX site itself since DPI inhibition of [^{3}H]BTXB binding is of the mixed type, DPI affecting the K_d and B_{max} values for [^{3}H]BTXB binding. This conclusion was confirmed by the fact that DPI accelerates the dissociation of [^{3}H]BTXB from its receptor site: $t_{1/2}$ is 87 min and 18 min for [^{3}H]BTXB dissociation from its site in the absence and in the presence of 10 μM DPI 201-106, respectively (not shown), a property that is not expected in a competitive inhibition. The most probable conclusion is that DPI has its own binding site that controls [^{3}H]BTXB binding allosterically. Although *S*-DPI and *R*-DPI have very different effects on the Na^+ channel, their binding properties are very similar with dissociation constants K_d of 100 nM. Since *R*- and *S*-DPI and local anesthetics (28) have similar effects on [^{3}H]BTXB binding, DPI might act at the local anesthetic's receptor site.

$^{22}Na^+$ flux studies with the different cell types used in this work have shown the following points. (*i*) Although *S*-DPI "activated" Na^+ channels in neuroblastoma cells and rat cardiac cells (Fig. 2), it did not stimulate sufficiently $^{22}Na^+$ uptake to identify an *S*-DPI-induced component over the background $^{22}Na^+$ uptake (Fig. 5). The same observation had been made with polypeptide toxins (20, 29) that also slow down (but do not block, unlike BTX or veratridine) Na^+ channel inactivation. (*ii*) *S*-DPI and *R*-DPI inhibited $^{22}Na^+$ entry through the Na^+ channel that had been activated by BTX (or by veratridine or by a mixture of veratridine and sea anemone toxin). DPI inhibition of $^{22}Na^+$ uptake through toxin-activated Na^+ channels was observed in the same range of concentrations for the *R* and *S* enantiomers. (*iii*) *S*-DPI and *R*-DPI had nearly identical effects on the different cell types that have been investigated.

Since neither the antagonist *R*-DPI nor the agonist *S*-DPI has any effect on the basal $^{22}Na^+$ uptake in the absence of BTX and since both enantiomers and the racemic mixture DPI 201-106 inhibit BTX binding to its site, all DPI molecules were of course expected to inhibit BTX-induced $^{22}Na^+$ influx through the Na^+ channel, as observed in Fig. 5.

The different cell types used in $^{22}Na^+$ flux studies have Na^+ channels that differ widely in their sensitivity to TTX and sea anemone toxins. Chicken cardiac cells and neuroblastoma cells are TTX-sensitive and relatively resistant to sea anemone toxins. Rat cardiac and skeletal muscle cells are resistant to TTX and sensitive to sea anemone toxins. C_9 cells have an intermediary position (13). In spite of the fact that these different subtypes of Na^+ channels have different pharmacological properties, they all seem to be nearly identical in their interaction with *S*- and *R*-DPI ($K_d \simeq 100$ nM). Unlike scorpion and sea anemone toxins (ref. 20 and Fig. 1), DPI is cardiotonic without being arrhythmogenic. The *S* enantiomer is responsible for the cardiotonic properties of the racemic mixture, probably by way of the same sequence of events that makes polypeptide toxins cardiotonic (20)—i.e., a slowing down of Na^+ channel inactivation → an increase in internal Na^+ concentration → an activation of the Na^+/Ca^{2+} exchanger accompanied by Ca^{2+} entry → an increased contraction.

We are very grateful to Dr. J. W. Daly for providing BTX, to Dr. J. R. Giglio for the generous gift of TiTxγ, to M. T. Ravier and N. Boyer for technical assistance, and to M. Valetti for secretarial assistance. This work was supported by the Centre National de la Recherche Scientifique and the Fondation pour la Recherche Médicale.

1. Scholtysik, G., Salzmann, R., Berthold, R., Herzig, J. W., Quast, U. & Markstein, R. (1985) *Naunyn-Schmiedebergs Arch. Pharmacol.* **329,** 316–325.
2. Buggisch, D., Isenberg, G., Ravens, U. & Scholtysik, G. (1985) *Eur. J. Pharmacol.* **118,** 303–311.
3. Kohlhardt, M., Fröbe, U. & Herzig, J. W. (1986) *J. Membr. Biol.* **89,** 163–172.
4. Narahashi, T. (1974) *Physiol. Rev.* **54,** 813–889.
5. Catterall, W. A. (1980) *Annu. Rev. Pharmacol. Toxicol.* **20,** 15–43.
6. Lazdunski, M. & Renaud, J. F. (1982) *Annu. Rev. Physiol.* **44,** 463–473.
7. Lazdunski, M., Frelin, C., Barhanin, J., Lombet, A., Meiri, H., Pauron, D., Romey, G., Schmid, A., Vigne, P. & Vijverberg, H. P. M. (1986) *Ann. N.Y. Acad. Sci.*, in press.
8. Chicheportiche, R., Balerna, M., Lombet, A., Romey, G. & Lazdunski, M. (1980) *Eur. J. Biochem.* **104,** 617–625.
9. Morrison, M. & Bayse, G. S. (1970) *Biochemistry* **9,** 2995–3000.
10. Vincent, J. P., Balerna, M., Barhanin, J., Fosset, M. & Lazdunski, M. (1980) *Proc. Natl. Acad. Sci. USA* **77,** 1646–1650.
11. Abita, J. P., Chicheportiche, R., Schweitz, H. & Lazdunski, M. (1977) *Biochemistry* **16,** 1838–1844.
12. Creveling, C. R., McNeal, E. T., Daly, J. W. & Brown, G. B. (1983) *Mol. Pharmacol.* **23,** 350–358.
13. Frelin, C., Vigne, P., Schweitz, H. & Lazdunski, M. (1984) *Mol. Pharmacol.* **26,** 70–74.
14. Lombet, A., Kazazoglou, T., Delpont, E., Renaud, J. F. & Lazdunski, M. (1983) *Biochem. Biophys. Res. Commun.* **110,** 894–901.
15. Barhanin, J., Giglio, J. R., Leopold, P., Schmid, A., Sampaio, S. V. & Lazdunski, M. (1982) *J. Biol. Chem.* **257,** 12553–12558.
16. Hampton, R. Y., Medzihradsky, F., Woods, J. H. & Dahlstrom, P. J. (1982) *Life Sci.* **30,** 2147–2154.
17. Renaud, J. F., Scanu, A. M., Kazazoglou, T., Lombet, A., Romey, G. & Lazdunski, M. (1982) *Proc. Natl. Acad. Sci. USA* **79,** 7768–7772.
18. Bordes, M., Bernengo, J. C. & Renaud, J. F. (1983) *Rev. Sci. Instrum.* **54,** 1053–1058.
19. Hamill, O., Marty, A., Neher, E., Sakmann, B. & Sigworth, F. J. (1981) *Pflügers Arch.* **391,** 85–100.
20. Romey, G., Renaud, J. F., Fosset, M. & Lazdunski, M. (1980) *J. Pharmacol. Exp. Ther.* **213,** 607–615.
21. Renaud, J. F., Kazazoglou, T., Lombet, A., Chicheportiche, R., Jaimovich, E., Romey, G. & Lazdunski, M. (1983) *J. Biol. Chem.* **258,** 8799–8805.
22. Ray, R., Morrow, C. S. & Catterall, W. A. (1978) *J. Biol. Chem.* **253,** 7307–7313.
23. Honerjager, P. (1982) *Rev. Physiol. Biochem. Pharmacol.* **92,** 1–74.
24. Brody, T. M. & Akera, T. (1984) in *Physiology and Pathophysiology of the Heart*, ed. Sperelakis, N. (Nijhoff, Boston), pp. 405–419.
25. Hof, R. P., Rüegg, U. T., Hof, A. & Vogel, A. (1985) *J. Cardiovasc. Pharmacol.* **7,** 689–693.
26. Franckowiak, G., Bechem, M., Schramm, M. & Thomas, G. (1985) *Eur. J. Pharmacol.* **114,** 223–226.
27. Catterall, W. A., Morrow, C. S., Daly, J. W. & Brown, G. B. (1981) *J. Biol. Chem.* **256,** 8922–8927.
28. Postma, S. W. & Catterall, W. A. (1984) *Mol. Pharmacol.* **25,** 219–227.
29. Jacques, Y., Fosset, M. & Lazdunski, M. (1978) *J. Biol. Chem.* **253,** 7383–7392.
30. Thormann, J., Kramer, W., Kremer, F. R. & Schlepper, M. (1986) *J. Cardiovasc. Pharmacol.* **8,** 749–757.